

The proton-air inelastic cross-section measurement at $\sqrt{s} \approx 2$ TeV from EAS-TOP experiment

G. C. Trinchero, M. Aglietta, A. Castellina, E. Cantoni, W. Fulgione, P. L. Ghia,* G. Mannocchi, C. Morello, P. Vallania, and S. Vernetto

Istituto di Fisica dello Spazio Interplanetario (INAF), I-10133 Torino, Italy and

Istituto Nazionale di Fisica Nucleare, I-10125 Torino, Italy

B. Alessandro

Istituto Nazionale di Fisica Nucleare, I-10125 Torino, Italy

P. Antonioli

Istituto Nazionale di Fisica Nucleare, I-40126 Bologna, Italy

F. Arneodo

Laboratori Nazionali del Gran Sasso, INFN, I-67010 Assergi (AQ), Italy

L. Bergamasco, M. Bertaina, A. Chiavassa, P. Galeotti, G. Navarra,† O. Saavedra, and C. Vigorito

Dipartimento di Fisica Generale dell'Università and INFN, I-10125 Torino, Italy

B. D'Ettorre Piazzoli, G. Di Sciascio,‡ and M. Iacovacci

Dipartimento di Scienze Fisiche dell'Università and INFN, I-80126 Napoli, Italy

The proton-air inelastic cross section value $\sigma_{p\text{-air}}^{\text{inel}} = 338 \pm 21(\text{stat}) \pm 19(\text{syst}) - 28(\text{syst})$ mb at $\sqrt{s} \approx 2$ TeV has been measured by the EAS-TOP Extensive Air Shower experiment. The absorption length of cosmic ray proton primaries cascades reaching the maximum development at the observation level is obtained from the flux attenuation for different zenith angles (i.e. atmospheric depths). The analysis, including the effects of the heavier primaries contribution and systematic uncertainties, is described. The experimental result is compared with different high energy interaction models and the relationships with the pp ($\bar{p}p$) total cross section measurements are discussed.

1. Introduction

This energy region $\sqrt{s} \approx 2$ TeV is of particular relevance because of high energy physics and astrophysics issues.

The pp total cross section, σ_{pp}^{tot} , and $\sigma_{p\text{-air}}^{\text{inel}}$ are related and can be inferred from each other by means of the Glauber theory. The whole procedure is model dependent, the results [1–5] differing of about 20% for \sqrt{s} values in the TeV energy range. Available accelerators' measurements at the highest energies, are themselves affected by systematic uncertainties of difficult evaluation. The pp ($\bar{p}p$) cross section measurements at energies of $\sqrt{s} = 1.8$ TeV [6–8] differ of about 10%, exceeding the statistical uncertainties of the measurements. It is therefore of primary interest to have experimental measurements of $\sigma_{p\text{-air}}^{\text{inel}}$ and σ_{pp}^{tot} at the same center of mass energy, i.e. around $\sqrt{s} \approx 2$ TeV, at which collider data are available.

The interpretation of Extensive Air Shower measurements relies on simulations that use hadronic interaction models based on theoretically guided extrapolations of the accelerator data obtained at lower en-

ergies and restricted to limited kinematical regions. A $\sigma_{p\text{-air}}^{\text{inel}}$ direct measurement and the comparison of observables as obtained from measurements and model based simulations, in the same conditions, is therefore highly recommended in order to confirm the validity of the whole analysis procedure.

Measurements of the p -air inelastic cross section performed in EAS have been reported. Since air shower detectors cannot observe the depth of the first interaction of the primary particle, indirect methods have to be used. Two main techniques are used: the constant N_e - N_μ cuts [10–12] by means of particle arrays, and the study of the shower longitudinal profiles using fluorescence detectors [13, 14] at higher energies.

Following the particle array technique, the primary energy is first selected by means of the muon number (N_μ). Proton induced showers at the same development stage are then selected by means of the shower size (N_e). The cross section of primary particles is obtained by studying the absorption in the atmosphere (λ_{obs}) of such showers, through their angular distribution at the observation level. The rate of showers decreases exponentially with zenith angle θ (i.e. atmospheric depth of first interaction) as:

$$f(\theta) = G(\theta)f(0)\exp[-x_0(\sec\theta - 1)/\lambda_{\text{obs}}] \quad (1)$$

where x_0 is the vertical atmospheric depth of the detector, and $G(\theta)$ the angular acceptance.

With air fluorescence detectors, the absorption length λ_{obs} is obtained fitting the atmospheric depth

*Present address: Laboratoire de Physique Nucleaire et de Hautes Energies, Universit s Paris 6 et Paris 7, CNRS-IN2P3, France

†Deceased

‡Present address: Istituto Nazionale di Fisica Nucleare, Tor Vergata, I-00133 Roma, Italy

of the maximum shower development stage (X_{max}) distribution tail.

The observed absorption length in both cases is affected by the fluctuations in the longitudinal development of the cascades and in the detector response. Such fluctuations can be studied through simulations, providing the conversion factor k between the observed absorption length and the interaction length of primary protons ($k = \lambda_{obs}/\lambda_{int}$). This factor is then used to convert the observed experimental absorption length λ_{obs}^{exp} into the interaction one λ_{int}^{exp} .

In this paper we will report on the measurement of the p -air inelastic cross section at primary energy $E_0 \approx 2 \cdot 10^{15}$ eV (i.e. $E_0 = (1.5 \div 2.5) \cdot 10^{15}$ eV, $\sqrt{s} \approx 2$ TeV) with the EAS-TOP experiment. Primary energies are below the steepening (*knee*) of the primary spectrum (i.e. $E_0 < 3 \cdot 10^{15}$ eV) above which the proton flux is strongly reduced. The constant N_e - N_μ analysis has been optimized [11] selecting showers at the maximum development stage where fluctuations are lower and heavier primaries rejection is improved by the request of the highest N_e values at a given primary energy.

The constant N_e - N_μ method with the selection of cascades' maximum development stage is equivalent to the study of X_{max} distribution tail. As shown in Fig. 1, the accessible part of the X_{max} distribution tail depends from the vertical atmospheric depth (x_0) of the detector. This is a limitation on the possibility to exploit this method at different atmospheric depths and on the maximum zenith angle θ (i.e. atmospheric depth) that can be considered in the analysis without running out of statistics. Systematic uncertainties of the measurement and the effect of possible contributions of heavier primaries are discussed and evaluated.

2. The experiment and the simulation

The EAS-TOP array was located at Campo Imperatore, Gran Sasso National Laboratory, 2005 m a.s.l., 820 g/cm² atmospheric depth.

The e.m. detector was made of 35 modules 10 m² each of plastic scintillators, 4 cm thick, distributed over an area of 10⁵ m². The trigger is fully efficient for $N_e > 10^5$, i.e. for primary proton energies $E_0 > 3 \cdot 10^{14}$ eV. The experimental resolutions for $N_e > 2 \cdot 10^5$ are: $\sigma_{N_e}/N_e \simeq 0.1$; $\sigma_{X_c} = \sigma_{Y_c} \simeq 5$ m; $\sigma_s \simeq 0.1$. The arrival direction of the shower is measured from the times of flight among the modules with resolution $\sigma_\theta \simeq 0.9^\circ$.

The muon-hadron detector (MHD), located at one edge of the e.m. array, is used, for the present analysis, as a tracking module with 9 active planes. Each plane includes two layers of streamer tubes (12 m length, 3×3 cm² section) and is shielded by 13 cm of iron. The total area of the detector is 12×12 m². A muon track is defined by the alignment of at least 6 fired

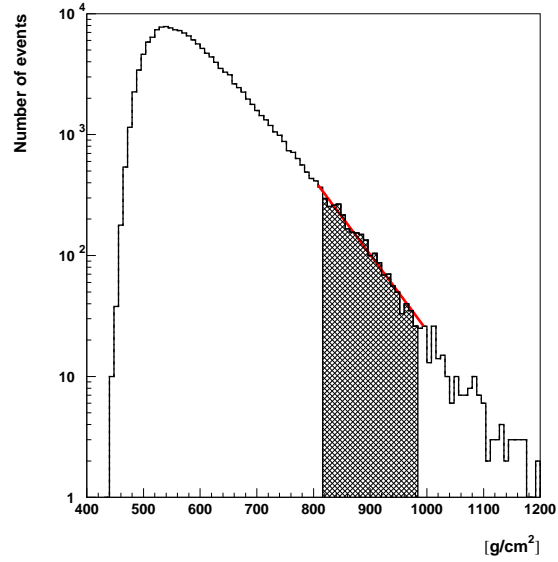


Figure 1: Depth of shower maximum (X_{max}) distribution for proton showers simulated with QGSJET II in the selected energy range ($E_0 = (1.5 \div 2.5) \cdot 10^{15}$ eV). The shaded area represents the interval of atmospheric depths (i.e. $1.0 \leq \sec \theta \leq 1.2$) considered in the analysis.

wires in different streamer tube layers leading to an energy threshold of $E_\mu^{th} \approx 1$ GeV.

A detailed description of the performance of the e.m. detector and of the muon-hadron detector can be found in Ref. [15, 16].

EAS simulations are performed with the CORSIKA program [17] with QGSJET II.03 [18] and SIBYLL 2.1 [19] high energy hadronic interaction models. These models have been widely employed for simulating atmospheric shower developments and have shown to provide consistent descriptions of different shower parameters in the considered energy range. Hadrons with energies below 80 GeV are treated with the GHEISHA 2002 interaction model.

Proton and Helium showers have been simulated with an energy threshold of 10¹⁵ eV, spectral index $\gamma = 2.7$ ($\gamma_{He} = 2.65$) up to $2 \cdot 10^{16}$ eV. KASCADE-like spectra [9] (resulting from our own fits) have been afterward sampled [11].

Simulated events have been analyzed using the same procedure followed for experimental data.

3. The analysis

The rate of showers of given primary energy ($E_{0,1} < E_0 < E_{0,2}$) selected through their muon number N_μ ($N_{\mu,1} < N_\mu < N_{\mu,2}$) and shower size N_e corresponding to maximum development ($N_{e,1} < N_e < N_{e,2}$) is measured.

The physical quantities required for the analysis are obtained through simulations, based on QGSJET II and SIBYLL interaction models, as described below.

Events in the specific proton primary energy range ($E_0 = (1.5 \div 2.5) \cdot 10^{15}$ eV) are selected by means of a matrix of minimum ($N_{\mu,1}$) and maximum ($N_{\mu,2}$) detected muon numbers for every possible combination of zenith angle and core distance from the muon detector. The selection table is obtained from simulated data for 5 m bins in core distance ($50 \text{ m} \leq r \leq 100 \text{ m}$) and $0.025 \text{ sec } \theta$ bins ($1.0 \leq \text{sec } \theta \leq 1.2$) for zenith angle. The selection of proton initiated cascades near maximum development is based on simulated distributions of the shower sizes at maximum development N_e^{max} in the selected energy interval. Choosing the shower size interval $\overline{\text{Log} N_e^{max}} \pm \sigma_{\text{Log} N_e^{max}}$ (i.e. $6.01 < \text{Log } N_e < 6.17$ for both interaction models) provides the selection of about 65% of the events around the maximum of the N_e^{max} distribution.

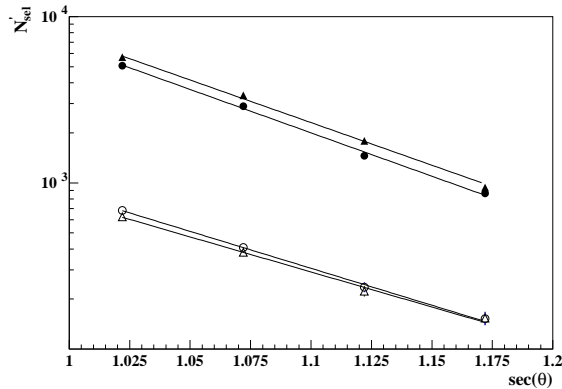


Figure 2: Acceptance corrected number of events vs. $\text{sec } \theta$ for the simulated (solid circle for QGSJET II and solid triangle for SIBYLL) and experimental data selected with the N_{μ} - N_e cuts calculated with the two interaction models (open circle for QGSJET II and open triangle for SIBYLL). The fits with expression (1) providing the λ_{obs} values are also shown (continuous lines).

The interaction length λ_{int}^{sim} is obtained as the average proton interaction depth in the selected energy range, it results to be $\lambda_{int}^{sim} = 60.3 \pm 0.1 \text{ g/cm}^2$ for QGSJET II and $\lambda_{int}^{sim} = 59.4 \pm 0.1 \text{ g/cm}^2$ for SIBYLL.

The acceptance corrected numbers of selected events N_{sel}' vs. zenith angle are shown in Fig. 2. The fit with expression (1) provides $\lambda_{obs}^{sim} = 68.5 \pm 1.4 \text{ g/cm}^2$ for QGSJET II and $\lambda_{obs}^{sim} = 69.9 \pm 1.4 \text{ g/cm}^2$ for SIBYLL. Therefore $k = \lambda_{obs}^{sim} / \lambda_{int}^{sim} = 1.14 \pm 0.02$ for QGSJET II and $k = 1.18 \pm 0.02$ for SIBYLL.

4. Results

The same analysis procedure discussed for the simulations is applied to the experimental data. The corresponding event numbers as a function of $\text{sec } \theta$ are also shown in Fig. 2, together with their fits providing $\lambda_{obs}^{exp} = 80.2 \pm 4.3 \text{ g/cm}^2$ and $\lambda_{obs}^{exp} =$

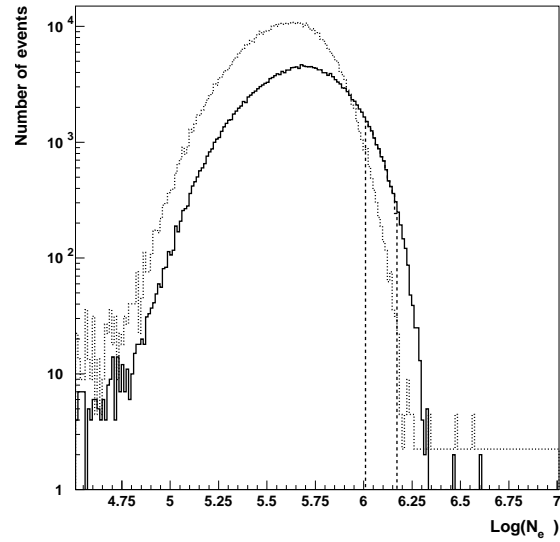


Figure 3: Shower size distribution ($\text{Log}(N_e)$) for proton (continuous) and helium (dotted) showers simulated with QGSJET II in the selected energy range. The two vertical dashed lines delimitate the $\text{Log}(N_e)$ interval considered in the analysis.

$84.7 \pm 5.0 \text{ g/cm}^2$ for QGSJET II and SIBYLL respectively. From the relation $\lambda_{int}^{exp} = \lambda_{obs}^{exp} / k$, we obtain $\lambda_{int}^{exp} = \lambda_{p-air} = 70.7 \pm 4.2 \text{ g/cm}^2$ for QGSJET II and $\lambda_{int}^{exp} = \lambda_{p-air} = 71.8 \pm 4.5 \text{ g/cm}^2$ for SIBYLL. The p -air inelastic cross section is then obtained from the relation $\sigma_{p-air}^{inel}(\text{mb}) = 2.41 \cdot 10^4 / \lambda_{p-air}$, and results to be $\sigma_{p-air}^{inel} = 341 \pm 20 \text{ mb}$ with QGSJET II and $\sigma_{p-air}^{inel} = 336 \pm 21 \text{ mb}$ with SIBYLL analysis.

The contribution of heavier nuclei has been evaluated by simulating helium primaries with QGSJET II, assuming the KASCADE spectrum and composition, which accounts for an helium flux about twice that of the protons in the energy range of interest but, as shown in Fig. 3, due to the high N_e values requested in our analysis, the helium contamination is reduced to less than 25%. The overall simulated observed absorption length becomes $\lambda_{obs}^{sim(p+He)} = 62.6 \pm 1.0 \text{ g/cm}^2$, which implies $k^{(p+He)} = 1.04 \pm 0.02$, and $\sigma_{p-air}^{inel} = 312 \pm 17 \text{ mb}$. Heavier primaries (i.e. CNO) hardly pass the N_{μ} - N_e cuts.

The analysis procedure based on one interaction model has been applied to a simulated experimental data set produced with a different interaction model with known p -air inelastic cross section in order to evaluate the systematic uncertainties. The result of the data simulated with SIBYLL ($\sigma_{p-air}^{inel} = 406 \pm 1 \text{ mb}$) when analyzed with QGSJET II is $\sigma_{p-air}^{inel} = 393 \pm 11 \text{ mb}$ ($\Delta \sigma_{p-air}^{inel} = -13 \pm 11 \text{ mb}$) and viceversa $\sigma_{p-air}^{inel} = 419 \pm 12 \text{ mb}$ when the data simulated with QGSJET II ($\sigma_{p-air}^{inel} = 400 \pm 1 \text{ mb}$) are analyzed with SIBYLL ($\Delta \sigma_{p-air}^{inel} = +19 \pm 12 \text{ mb}$).

An experimental data set has been simulated using QGSJET II with HDPM [20] cross section value

($\sigma_{p\text{-air}}^{\text{inel}} = 367 \pm 1$ mb) in order to check the capability to discriminate between two different values of the p -air cross section within the same interaction model. The lower cross section value is clearly discriminated by the analysis based on SIBYLL that gives $\sigma_{p\text{-air}}^{\text{inel}} = 372 \pm 13$ mb ($\Delta\sigma_{p\text{-air}}^{\text{inel}} = -5 \pm 13$ mb). The differences between the simulated and measured values ($\Delta\sigma_{p\text{-air}}^{\text{inel}}$) are both positive and negative and compatible with the statistical uncertainties. Therefore we define as maximum systematic uncertainty the value $\sigma_{\text{syst}} = 19$ mb which provides the χ^2 value corresponding to 99% C.L for the distribution of the four deviations $\Delta\sigma_{p\text{-air}}^{\text{inel}}$.

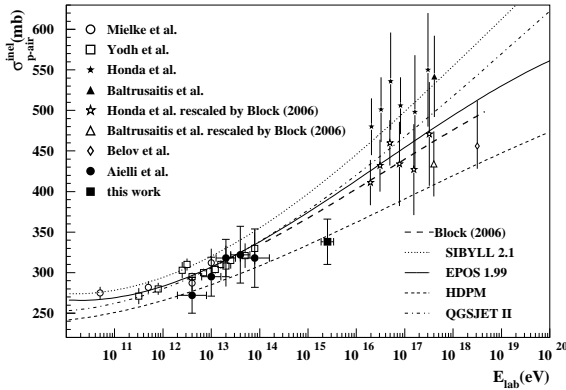


Figure 4: p -air inelastic cross section data including the present measurement (solid square), and different hadronic interaction models.

5. Conclusions

Combining the results obtained with the two considered interaction models and including the systematic uncertainties the p -air inelastic cross section is:

$$\sigma_{p\text{-air}}^{\text{inel}} = 338 \pm 21_{\text{stat}} \pm 19_{\text{syst}} - 29_{\text{syst}}(\text{He}) \text{ mb}$$

As shown in Fig. 4, this value is about 15% smaller than the values in use within QGSJET II and SIBYLL and in better agreement with Refs. [4, 20, 21]. Predicted $\sigma_{p\text{-air}}^{\text{inel}}$ values, obtained from different σ_{pp}^{tot} Tevatron measurements at $\sqrt{s} = 1.8$ TeV by using different calculations based on the Glauber theory, are reported in Fig. 5. The present measurement is consistent with smaller values of the $\bar{p}p$ total cross section ($\sigma_{pp}^{\text{tot}} = 72.8 \pm 3.1$ mb [7], and $\sigma_{pp}^{\text{tot}} = 71 \pm 2$ mb [8]), and the pp to p -air calculations predicting for a given value of σ_{pp}^{tot} , a smaller value of $\sigma_{p\text{-air}}^{\text{inel}}$ [4, 5]. Independently from the cross section analysis, the measured values of the absorption length λ_{obs} are about 15% higher than the simulated ones for both the considered interaction models. This can be probably ascribed to the fact that the measured cascades penetrate deeper into the atmosphere than predicted by the interaction models.

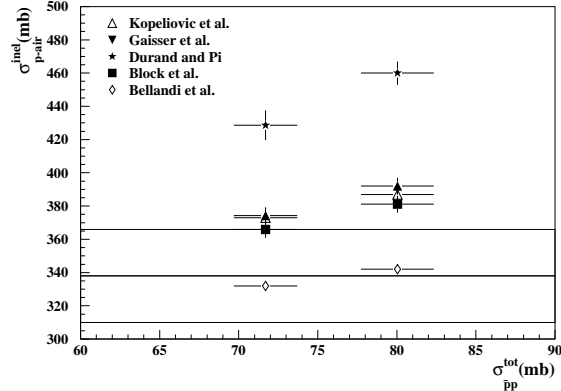


Figure 5: p -air inelastic vs. $\bar{p}p$ total cross section data. The present result (± 1 s.d., solid lines) is shown together with the results of different calculations derived from $\bar{p}p$ measurements reported at $\sqrt{s} = 1.8$ TeV.

References

- [1] T. K. Gaisser, U. P. Sukhatme, G. B. Yodh, Phys. Rev. D, **36** (1987) 1350.
- [2] L. Durand and H. Pi, Phys. Rev. D, **38** (1988) 78-84
- [3] B. Z. Kopeliovich, B.Z. Nikolaev, I.K. Potashnikova, Phys. Rev. D, **39** (1989) 769-779.
- [4] M. M. Block, Phys. Rep., **436** (2006) 71-215.
- [5] J. Bellandi et al., Phys. Lett. B **343** (1995) 410.
- [6] F. Abe et al., Phys. Rev. D, **50** (1994) 5550.
- [7] N. A. Amos et al., Phys. Lett. B, **243** (1990) 158.
- [8] C. Avila et al., Phys. Lett. B, **445** (1999) 419.
- [9] T. Antoni et al, Astropart. Phys., **24** (2005) 1-25.
- [10] M. Honda et al., Phys. Rev. Lett., **70** (1993) 525.
- [11] M. Aglietta et al., Phys. Rev. D, **79** (2009) 032004.
- [12] G. Aielli et al., Phys. Rev. D, **80** (2009) 092004.
- [13] R. M. Baltrusaitis et al., Phys. Rev. Lett., **52** (1984) 1380.
- [14] K. Belov et al., Nucl. Phys. Proc. Suppl., **151** (2006) 197-204.
- [15] M. Aglietta et al., Nucl. Inst. Meth. Phys. Res. A, **336** (1993) 310.
- [16] R. Adinolfi et al., Nucl. Inst. Meth. Phys. Res. A, **420** (1999) 117.
- [17] D. Heck et al., Report **FZKA 6019**, Forschungszentrum Karlsruhe (1998).
- [18] S. Ostapchenko, Phys. Rev. D, **74** (2006) 014026.
- [19] R. Engel et al. Proc. 26th Int. Cosmic Ray Conf., Salt Lake City (USA), **1** (1999) 415.
- [20] J. N. Capdevielle, J. Phys. G: Nucl. Part. Phys. **15** (1989) 909.
- [21] J.R. Hörandel, J. Phys. G: Nucl. Part. Phys. **29** (2002) 2439